STEAM-H: Science, Technology, Engineering, Agriculture, Mathematics & Health

Martha Refugio Ortiz-Posadas *Editor*

Pattern Recognition Techniques Applied to Biomedical Problems

Springer

STEAM-H: Science, Technology, Engineering, Agriculture, Mathematics & Health

STEAM-H: Science, Technology, Engineering, Agriculture, Mathematics & Health

Series Editor
Bourama Toni
Department of Mathematics
Howard University
Washington, DC, USA

This interdisciplinary series highlights the wealth of recent advances in the pure and applied sciences made by researchers collaborating between fields where mathematics is a core focus. As we continue to make fundamental advances in various scientific disciplines, the most powerful applications will increasingly be revealed by an interdisciplinary approach. This series serves as a catalyst for these researchers to develop novel applications of, and approaches to, the mathematical sciences. As such, we expect this series to become a national and international reference in STEAM-H education and research.

Interdisciplinary by design, the series focuses largely on scientists and mathematicians developing novel methodologies and research techniques that have benefits beyond a single community. This approach seeks to connect researchers from across the globe, united in the common language of the mathematical sciences. Thus, volumes in this series are suitable for both students and researchers in a variety of interdisciplinary fields, such as: mathematics as it applies to engineering; physical chemistry and material sciences; environmental, health, behavioral and life sciences; nanotechnology and robotics; computational and data sciences; signal/image processing and machine learning; finance, economics, operations research, and game theory.

The series originated from the weekly yearlong STEAM-H Lecture series at Virginia State University featuring world-class experts in a dynamic forum. Contributions reflected the most recent advances in scientific knowledge and were delivered in a standardized, self-contained and pedagogically-oriented manner to a multidisciplinary audience of faculty and students with the objective of fostering student interest and participation in the STEAM-H disciplines as well as fostering interdisciplinary collaborative research. The series strongly advocates multidisciplinary collaboration with the goal to generate new interdisciplinary holistic approaches, instruments and models, including new knowledge, and to transcend scientific boundaries.

More information about this series at http://www.springer.com/series/15560

Martha Refugio Ortiz-Posadas
Editor

Pattern Recognition Techniques Applied to Biomedical Problems

Springer

Editor
Martha Refugio Ortiz-Posadas
Electrical Engineering Department
Universidad Autónoma
Metropolitana-Iztapalapa
Mexico City, Mexico

ISSN 2520-193X ISSN 2520-1948 (electronic)
STEAM-H: Science, Technology, Engineering, Agriculture, Mathematics & Health
ISBN 978-3-030-38020-5 ISBN 978-3-030-38021-2 (eBook)
https://doi.org/10.1007/978-3-030-38021-2

Mathematics Subject Classification: 65D18, 92Bxx, 68T10, 68T30, 68T35

This Springer imprint is published by the registered company Springer Nature Switzerland AG.
The registered company address is: Gewerbestrasse 11, 6330 Cham, Switzerland

Preface

Pattern recognition is the science that studies the processes of identification, characterization, classification, and reconstruction of sets of objects or phenomena, with the purpose of extracting information that allows establishing common properties among them. It has an applied and multidisciplinary character, and it is conformed to technical sciences, computer science, and mathematics, among others, in order to develop computational tools and methodologies related to these processes. The fundamental problems of pattern recognition refer to those related to the determination of factors that affect objects and their classification, and four types are considered: (1) selection of variables and objects, (2) supervised classification, (3) unsupervised classification, and (4) partially supervised classification.

On the other hand, there are different study areas of pattern recognition such as image processing, signal processing, computer vision, remote sensing, neural networks, genetic algorithms, artificial intelligence techniques, descriptive geometry, mathematical morphology, statistical recognition, structural syntactic recognition, and combinatorial logical recognition, to name a few. All these can be applied into biomedical problems.

This volume presents together leading Latin American researchers from five different countries, namely, Brazil, Chile, Costa Rica, México, and Uruguay, to present their own work with the perspective to advance their specific fields. It presents nine chapters regarding different pattern recognition technics applied to the solution of several biomedical problems featured as follows.

In Chap. 1, Aída Jiménez-González and Norma Castañeda-Villa present two experiences on the recovery of physiological information from noisy datasets, applying the method of independent component analysis (ICA).

In Chap. 2, Verónica Jacinto Jiménez et al. describe the identification process of genomic variants and genetic expression profiles for the diagnostic of diseases using high-throughput sequencing methodologies.

In Chap. 3, Leticia Vega-Alvarado et al. propose a system for the automatic detection of the parasite causing Chagas disease in stained blood smears images.

In Chap. 4, Alfonso Rosales-López and Rosimary Terezinha de Almeida propose the use of intervention analysis on time series, using the Box and Tiao approach, as a method for health technology assessment on public health interventions.

In Chap. 5, Millaray Curilem et al. evaluate the possibility of detecting the presence of nausea in chemotherapy patients by processing the electrogastrogram signal.

In Chap. 6, Letícia M. Raposo et al. describe the random forest algorithm, showing an application to predict HIV-1 drug resistance.

In Chap. 7, Luis Jiménez-Ángeles et al. describe an overview of the medical imaging modalities most frequently used for assessment of the cardiac contraction pattern.

In Chap. 8, Franco Simini et al. describe two automatic systems related with home care and personal devices.

In Chap. 9, Tlazohtzin Mora-García et al. propose an evaluation tool based on multi-criteria decision analysis (MCDA) for the replacement of older medical equipment installed at hospitals.

Mexico City, Mexico Martha Refugio Ortiz-Posadas

Contents

Contributors

Rosimary Terezinha de Almeida Programa de Engenharia Biomédica, COPPE, Universidade Federal do Rio de Janeiro, Rio de Janeiro, Brazil

Pablo Álvarez-Rocha Universidad de la República, Montevideo, Uruguay

Alberto Caballero-Ruiz Instituto de Ciencias Aplicadas y Tecnología, Universidad Nacional Autónoma de México, Mexico City, Mexico
National Laboratory for Additive and Digital Manufacturing (MADiT), Mexico City, Mexico

Norma Castañeda-Villa Electrical Engineering Department, Universidad Autónoma Metropolitana-Iztapalapa, Mexico City, Mexico

Max Chacón Departamento de Ingeniería Informática, Universidad de Santiago de Chile, Santiago, Chile

Millaray Curilem Centro de Física e Ingeniería para la Medicina (CFIM), Universidad de La Frontera, Temuco, Chile

Mariano Flores Hospital Regional Dr. Hernán Henríquez Aravena, Temuco, Chile

Matías Galnares Universidad de la República, Montevideo, Uruguay

Laura Gómez-Romero Unidad de Servicios Bioinformáticos, Instituto Nacional de Medicina Genómica, Mexico City, Mexico

Francisco Heredia-López Centro de Investigaciones Regionales Dr. Hideyo Noguchi, Universidad Autónoma de Yucatán, Mérida, Mexico

Luis Jiménez-Ángeles Departamento de Ingeniería en Sistemas Biomédicos, Universidad Nacional Autónoma de México, Mexico City, Mexico

Aída Jiménez-González Electrical Engineering Department, Universidad Autónoma Metropolitana-Iztapalapa, Mexico City, Mexico

Verónica Jiménez-Jacinto Instituto de Biotecnología, Universidad Nacional Autónoma de México, Mexico City, Mexico

Richard Low Infor-Med Medical Information Systems Inc., Woodland Hills, CA, USA

Verónica Medina-Bañuelos Electrical Engineering Department, Universidad Autónoma Metropolitana-Iztapalapa, Mexico City, Mexico

Carlos-Francisco Méndez-Cruz Centro de Ciencias Genómicas, Universidad Nacional Autónoma de México, Mexico City, Mexico

Tlazohtzin R. Mora-García Electrical Engineering Department, Universidad Autónoma Metropolitana-Iztapalapa, Mexico City, Mexico

Flavio F. Nobre Programa de Engenharia Biomédica, Universidade Federal do Rio de Janeiro, Rio de Janeiro, Brazil

Gabriela Ormaechea Universidad de la República, Montevideo, Uruguay

Martha Refugio Ortiz-Posadas Electrical Engineering Department, Universidad Autónoma Metropolitana-Iztapalapa, Mexico City, Mexico

Fernanda Piña-Quintero Service of Electro-Medicine, National Institute of Pediatrics, Mexico City, Mexico

Letícia M. Raposo Programa de Engenharia Biomédica, Universidade Federal do Rio de Janeiro, Rio de Janeiro, Brazil

Paulo Tadeu C. Rosa Programa de Engenharia Biomédica, Universidade Federal do Rio de Janeiro, Rio de Janeiro, Brazil

Alfonso Rosales-López Gerencia de Infraestructura y Tecnología, Caja Costarricense de Seguro Social, San José, Costa Rica

Leopoldo Ruiz-Huerta Instituto de Ciencias Aplicadas y Tecnología, Universidad Nacional Autónoma de México, Mexico City, Mexico

Hugo Ruiz-Piña Centro de Investigaciones Regionales Dr. Hideyo Noguchi, Universidad Autónoma de Yucatán, Mérida, Mexico

Alejandro Santos-Díaz Departamento de Mecatrónica, Escuela de Ingenieria y Ciencias, Tecnológico de Monterrey, Campus Ciudad de México, Mexico City, Mexico

Gabriela Silvera Universidad de la República, Montevideo, Uruguay

Franco Simini Universidad de la República, Montevideo, Uruguay

Sebastián Ulloa Departamento de Ingeniería Eléctrica, Universidad de La Frontera, Temuco, Chile

Raquel Valdés-Cristerna Electrical Engineering Department, Universidad Autónoma Metropolitana-Iztapalapa, Mexico City, Mexico

Leticia Vega-Alvarado Instituto de Ciencias Aplicadas y Tecnología, Universidad Nacional Autónoma de México, Mexico City, Mexico

Claudio Zanelli Onda Corporation, Sunnyvale, CA, USA

The Classification of Independent Components for Biomedical Signal Denoising: Two Case Studies

Aída Jiménez-González and Norma Castañeda-Villa

Abstract This chapter presents two experiences on the recovery of biomedical signals of interest from noisy datasets, i.e., the extraction of the fetal phonocardiogram from the single-channel abdominal phonogram and the recovery of the Long Latency Auditory Evoked Potential from the multichannel EEG (in children with a cochlear implant). These by implementing denoising strategies based on (1) the separation of components statistically independent by using Independent Component Analysis (ICA) and, of especial interest in this chapter, (2) the classification of the components of interest by taking advantage of properties such as temporal structure, frequency content, or temporal and spatial location. Results of these two case studies are presented on real datasets, where either focused (1) on rhythmic physiological events such as the fetal heart sounds or (2) on spatially localized events like the cochlear implant artifact, the classification stage has been fundamental on the performance of the denoising process and thus, on the quality of the retrieved signals.

Keywords Blind source separation · Cochlear implant artifact · Fetal heart rate · Independent component analysis · TDSep

1 Introduction

During the last three decades, Independent Component Analysis (ICA) has been recognized as a powerful solution to the matter of revealing the driving forces that underlie a set of observed phenomena [1–3]. Particularly, ICA has been important in the field of biomedical signal processing, where the recovery of very low-amplitude signals from a set of mixtures has posed a challenge that traditional approaches

A. Jiménez-González (✉) · N. Castañeda-Villa
Electrical Engineering Department, Universidad Autónoma Metropolitana-Iztapalapa, México City, México
e-mail: aidaj@xanum.uam.mx

M. R. Ortiz-Posadas (ed.), *Pattern Recognition Techniques Applied to Biomedical Problems*, STEAM-H: Science, Technology, Engineering, Agriculture, Mathematics & Health, https://doi.org/10.1007/978-3-030-38021-2_1

like digital filtering do not manage to solve. This has been possible because of the development of multiple and efficient implementations of ICA that make it suitable to separate data that used to be thought as too difficult to process [4–8]. As a result, ICA has been successfully used for the extraction of information of interest from electroencephalographic [5, 9, 10], electrocardiographic [9, 11], and, more recently, electromyographic [12], magnetocardiographic [13, 14], magnetoencephalographic [15, 16], and phonographic recordings [17–20].

Results have been promising and have motivated further research into the development of new ICA algorithms and methodologies for performance evaluation that, while paying attention on high-quality separation (and evaluation) of the independent components (ICs) finally recovered, leave the researcher the responsibility of giving physical (or physiological) sense to them and thus to identify and select the components of interest. The task may sound easy at first, but due to the typical high dimensionality of the datasets (e.g., 7, 16, 19, 30, 36, 49, 50, 55, 64, 68, 128, or 130 channels and different recording lengths) and the usually unknown characteristics of the undesirable sources (both physiological and nonphysiological), it requires objective and, if possible, automatic alternatives that ease what we will refer to as the third step of the procedure for denoising biomedical signals by means of ICA, i.e., the classification of the ICs.

At present, different strategies have been presented in the literature, all dependent on the dataset and, certainly, on the experience of the authors, which illustrates the challenge behind the classification task for biomedical signal denoising. Here, we present our experience on two different sceneries: the extraction of the fetal heart sounds from the single-channel abdominal phonogram (i.e., by classifying rhythmic ICs associated to the fetal cardiac activity) and the elimination of the cochlear implant (CI) artifact from the multichannel EEG (i.e., by classifying independent components with artifactual activity synchronized with the acoustic stimulus and spatially located close to the cochlear implant position). To this end, this chapter is organized as follows: Section 2 presents the theoretical background of ICA, while Sects. 3 and 4, respectively, detail the sceneries for denoising the abdominal phonogram and the EEG along with their results and discussion. Finally, Sect. 5 presents our final remarks.

2 Independent Component Analysis

ICA is a statistical algorithm whose aim is to represent a set of mixed signals as a linear combination of statistically independent sources. This technique estimates ICs, denoted by $\hat{\mathbf{s}}(t)$, from a group of observations, $\mathbf{x}(t)$, which are considered as linear and instantaneous mixtures of unknown sources, $\mathbf{s}(t)$ [21]. The statement that in a biomedical signal different sensors/electrodes receive different mixtures of the sources is exploited by ICA, that is, spatial diversity. Spatial diversity means that ICA looks for structures across the sensors and not (necessarily) across time.

ICA identifies the probability distribution of the measurements, given a sample distribution [22].

In the most simplistic formulation of the ICA problem (noise-free), p measured signals $\mathbf{x}(t)$ are a linear mixture of unknown but statistically independent q sources $\mathbf{s}(t)$; each source has moments of any order, zero mean, and $p \geq q$. Then, the ICA model is as follows:

$$\mathbf{x}(t) = \mathbf{A}\,\mathbf{s}(t), \tag{1}$$

where the square mixing matrix $\mathbf{A}$ is also unknown but invertible, $\mathbf{x}(t) = [x_1, x_2, \ldots, x_p]^T$ and $\mathbf{s}(t) = [s_1, s_2, \ldots, s_q]^T$. ICA calculates the demixing matrix, $\mathbf{W} = \mathbf{A}^{-1}$, from the observations $\mathbf{x}(t)$ and estimates the original sources by a linear transform:

$$\hat{\mathbf{s}}(t) = \mathbf{W}\,\mathbf{x}(t), \tag{2}$$

where $\mathbf{W}$ is found by maximizing the statistical independence of the output components [23].

Currently, depending on the method used to seek statistical independence (i.e., higher-order statistics or time-structure-based algorithms), different ICA implementations have been developed. Among the wide range of ICA algorithms, three are frequently used in the field of biomedical signal processing: FastICA [24], Infomax [25, 26], and Temporal Decorrelation Source Separation (TDSep) [27]. The theory behind these three ICA algorithms will be explained in the next sections, all of them share steps (a) and (b) as the initial stage:

(a) *Centering*: Subtract the mean of the mixtures, which simplifies the ICA algorithm $\mathbf{x}(t) = \mathbf{x}(t) - E\{\mathbf{x}(t)\}$, where $E\{\mathbf{x}(t)\}$ is the mean vector of the measurements; when the algorithm is finished, the mean vector is added back.

(b) *Whitening or sphering*: In this preprocessing step, the covariance matrix is calculated as $\mathbf{R_{xx}} = E\{\mathbf{x}(t)\mathbf{x}^T(t)\}$, and then, an eigenvalue decomposition is performed on it; the decomposition is given by $\mathbf{R} = \mathbf{E}\Lambda\mathbf{E}^T$, where $\mathbf{E}$ is the orthonormal matrix of eigenvectors of $\mathbf{R}$, and Λ is the diagonal matrix of eigenvalues. Transforming the covariance matrix into an identity matrix, a whitening $\mathbf{M}$ matrix is calculated as $\mathbf{M} = (\Lambda^{1/2}\mathbf{E}^T)^{-1}$. This is also known as a principal component decomposition.

2.1 FastICA

This is a computationally efficient algorithm that uses simple estimators of negative entropy, $J(y)$, to search a $\mathbf{W}$ matrix that, when applied to mixtures, maximizes this property in the resulting components, thus allowing the estimation of sources with non-Gaussian probability distributions [28, 29]. It estimates ICs by following either the deflation approach (Defl), where the components are extracted one by one, or the

symmetric approach (Sym), where the components are simultaneously extracted. The negative entropy is defined as follows:

$$J(\boldsymbol{w}) = \left[E\left\{G\left(\boldsymbol{w}^T\boldsymbol{v}\right)\right\} - E\left\{G(\boldsymbol{v})\right\}\right]^2, \tag{3}$$

where $\boldsymbol{w}$ is an m-dimensional vector such as $E\{(\boldsymbol{w}^T\boldsymbol{v})^2\} = 1$, $\boldsymbol{v}$ is a Gaussian variable with zero mean and unit variance, and G is a nonquadratic cost function, e.g., tan$h$ or y^3. The problem is now reduced to find a transformation $\mathbf{W}$ whose vectors, $\boldsymbol{w}$, are iteratively adjusted to maximize J which is equivalent to reduce the mutual information (MI); this is performed by a fixed-point algorithm. From choosing an initial weight vector $\boldsymbol{w}$, the algorithm calculates the direction of $\boldsymbol{w}$ maximizing the non-Gaussianity of the projection $\boldsymbol{w}^T\boldsymbol{x}$ (linear combination of the measured signals). Since the signal is already whitened, to make the variance of $\boldsymbol{w}^T\boldsymbol{x}$ unity, it is sufficient to constrain the norm of the pseudo-inverse of the initial weight vector $\boldsymbol{w}^+$, to be unity, $\boldsymbol{w} = \boldsymbol{w}^+/\|\boldsymbol{w}^+\|$; if the old and new values of $\boldsymbol{w}$ do not point in the same direction, the algorithm recalculates the direction of $\boldsymbol{w}$. Finally, the demixing matrix is given by $\mathbf{W} = \boldsymbol{w}^T\mathbf{M}$ and the estimations $\hat{\mathbf{s}}(t)$ by Eq. 2.

2.2 Infomax and Ext-Infomax

Described by Bell and Sejnowski [25], Infomax is an ICA algorithm which uses the mutual information between the estimated sources as a criterion of the minimization of independence, with which the joint negative entropy is maximized. The demixing matrix $\mathbf{W}$, which is found using stochastic gradient ascent, maximizes the entropy of an input vector $\mathbf{x_G}$, linearly transformed $\mathbf{u} = \mathbf{W}\mathbf{x_G}$, and sigmoidally compressed $y = g(\mathbf{u})$. Then, $\mathbf{W}$ performs component separation while the nonlinear $g(.)$ provides the necessary high-order statistic information, $g(\mathbf{u}_i) = (1 + \exp(-\mathbf{u}_i))^{-1}$. This gives an update rule $\hat{\mathbf{u}}_i = 1 - 2\mathbf{u}_i$. *Infomax* is able to decompose signals into ICs with sub- and super-Gaussian distributions in its extended version. The original learning rule for super-Gaussian distributions is as follows:

$$\Delta\mathbf{W} \propto \left[\mathbf{I} - \tan h(\mathbf{u})\,\mathbf{u}^T - \mathbf{u}\mathbf{u}^T\right]\mathbf{W}, \tag{4}$$

where $\mathbf{I}$ is the identity matrix, and $\mathbf{u}$ are the estimated sources. The extended learning rule (Ext-Infomax) [26] for sub-Gaussian distributions is as follows:

$$\Delta\mathbf{W} \propto \left[\mathbf{I} - \boldsymbol{\Lambda}\tan h(\mathbf{u})\,\mathbf{u}^T - \mathbf{u}\mathbf{u}^T\right]\mathbf{W}. \tag{5}$$

The algorithm switches between two learning rules: one for sub-Gaussian and one for super-Gaussian sources. $\boldsymbol{\Lambda}$ is a diagonal matrix which includes the switching

criterion between the two learning rules: $\Lambda_{ij} = 1$ for super-Gaussian and -1 for sub-Gaussian. Finally, the estimated sources $\hat{\mathbf{s}}(t)$ are computed by Eq. 2.

2.3 TDSep

The Temporal Decorrelation Source Separation (TDSep) algorithm [27] takes into account the temporal structure of the signals. TDSep uses several time-delayed second-order correlation matrices for source separation. JADE and TDSep determinate the mixing matrix based on a joint approximate diagonalization of symmetric matrices; the principal difference between these two algorithms is that JADE maximizes the kurtosis of the signals, while TDSep minimizes temporal cross-correlation between the signals [30].

TDSep could be summarized as follows: firstly, Ziehe and Müller define a cost function based on a certain time lag τ and a time average that measure the correlation between the signals; after whitening, this cost function imposes decorrelation over time. After that, they propose an alternative technique for the joint diagonalization using a rotation [31]. In the rotation step, the cost function can be minimized by approximate simultaneous diagonalization of several correlation matrices through several elementary JACOBI rotations [22] to obtain the so-called rotation matrix, $\mathbf{Q}$.

TDSep computes those matrices relying only on second-order statistics and diagonalizes the covariance matrices $\mathbf{R}_{\mathbf{xx}}$ for a time lag $\tau = 0$ and at the same time diagonalizes the covariance matrix for a given delay $\mathbf{R}_{\mathbf{x}\tau} = E\{\mathbf{x}(t)\mathbf{x}(t-\tau)^T\}$. The source covariance matrix $\mathbf{R}_{\mathbf{s}\tau}$ is diagonal for all time lags $\tau = 0, 1, 2, \ldots, N-1$ as $\mathbf{R}_{\mathbf{s}\tau} = \mathbf{W}\mathbf{R}_{\mathbf{x}\tau}\mathbf{W}^T$, where $\mathbf{R}_{\mathbf{x}\tau}$ is the signal covariance matrix. This algorithm determines the mixing matrix based on a joint approximate digitalization of symmetric matrices. Finally, using the whitening matrix $\mathbf{M}$ and the rotation matrix $\mathbf{Q}$, an estimate of the mixing matrix can be calculated as follows:

$$\hat{\mathbf{A}} = \mathbf{M}^{-1}\mathbf{Q}, \tag{6}$$

and the estimations $\hat{\mathbf{s}}(t)$ by Eq. 2.

3 Case Study I: Denoising the Abdominal Phonogram

This first case describes a methodology for the recovery of the fetal heart sounds (i.e., the fetal phonocardiogram, FPCG) from the single-channel abdominal phonogram, which has been implemented by using a denoising strategy based on what has been referred to as single-channel ICA (SCICA) [17, 20, 32].

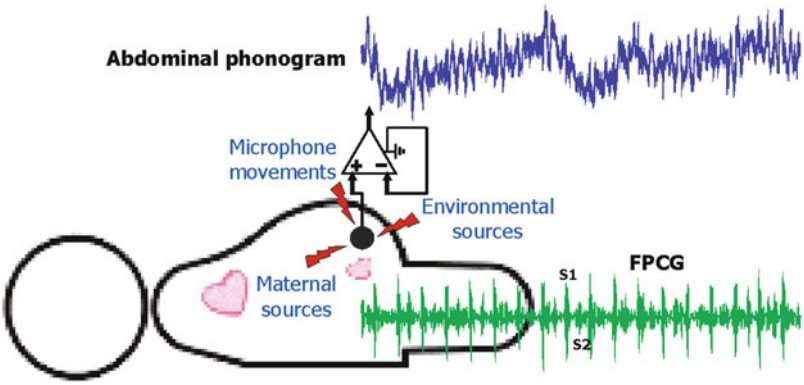

Fig. 1 Distortion of the FPCG by physiological and nonphysiological sources during the abdominal recording. The FPCG corresponds to the acoustic vibrations produced by the fetal heart, where the two main heart sounds (S1 and S2) are indicated. The abdominal phonogram, which is recorded by a microphone positioned on the maternal womb, is a mixture of multiple sources, where the fetal information is hardly noticed

3.1 The Problem Definition

During the last two decades, fetal examination by passive detection of cardiac vibrations has regained attention [17, 33–38]. The technique is performed by positioning a sensitive acoustic sensor on the maternal womb to record the abdominal phonogram, a signal that is rich in information for well-being assessment (i.e., it contains the two main fetal heart sounds S1 and S2, which can be used to estimate the heart rate and the heart valve condition) but highly attenuated by the amniotic fluid and abdominal tissues and, consequently, highly immersed (both temporally and spectrally) in maternal and environmental sources whose characteristics turn the recovery of fetal information into a challenging task. Fig. 1 illustrates the acoustic vibrations produced by the beating fetal heart (i.e., the FPCG, as a free of noise trace where the two main heart sounds, S1 and S2, can be detected) and the acoustic vibrations actually recorded at the surface of the maternal womb (i.e., the abdominal phonogram, where the fetal information is hard to observe).

In our work, as an alternative to the rigid approach given by traditional digital filtering schemes (which assume that the FPCG spectrum does not change, independently on the fetal age, heart rate, or condition), we have studied a data-driven strategy that, by taking advantage of the rich time-structure in the abdominal phonogram, adapts itself to each dataset to extract the fetal heart sounds from the abdominal phonogram (i.e., the FPCG) [17]. This approach, known as SCICA, has been applied to a set of 25 noisy single-channel abdominal phonograms. This first case study will describe such a dataset in Sect. 3.2, detail the implementation of SCICA for denoising purposes in Sect. 3.3, present our findings in Sect. 3.4, and, finally, a brief Discussion in Sect. 3.5.

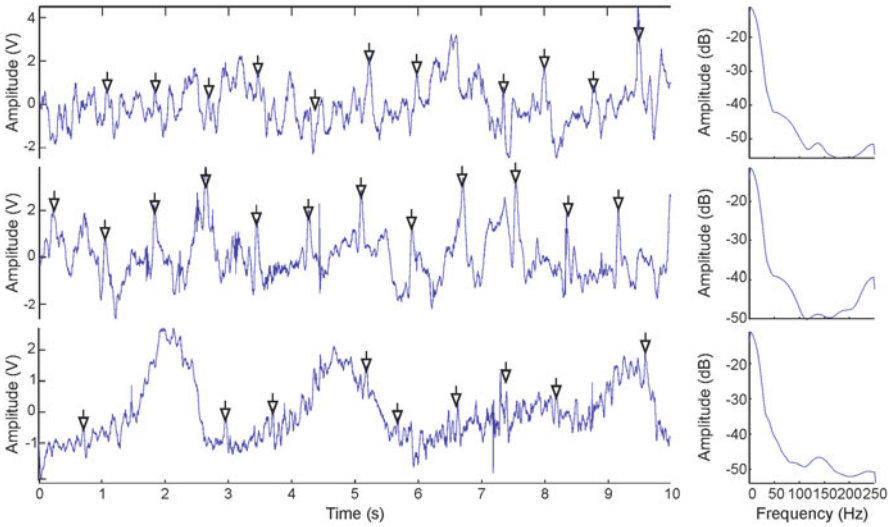

Fig. 2 Time (left-hand side) and frequency (right-hand side) representations of three abdominal phonograms in the dataset. (Modified from [39])

3.2 A Dataset of Single-Channel Abdominal Phonograms

The dataset is composed of 25 single-channel recordings that were digitized at a sampling frequency of 500 Hz during 3 or 5 minutes (MP100, Biopac Systems™). The data was obtained from 18 pregnant women (24 ± 3 years old and fetal gestational ages between 29 and 40 weeks, who provided their informed consent to participate in the study) by using a PCG piezoelectric transducer (TK-701T, Nihon Kohden™) connected to a general purpose amplifier (DA100, Biopac Systems™). Additionally, as a reference signal, the abdominal ECG was simultaneously recorded. Figure 2 presents segments (10 s length) of three abdominal phonograms in the dataset and their frequency content, where the signals clearly show a slow component along with some quasiperiodic peaks (indicated by downward arrows), but without any clear evidence of the FPCG.

3.3 Single-Channel ICA (SCICA)

The implementation of SCICA requires three stages [17, 32]: a preprocessing stage that projects the single-channel abdominal phonogram into a higher dimensional space, a processing stage that transforms such a multichannel representation into a set of multiple ICs, and, finally, a postprocessing stage that, in this case study, automatically classifies the rhythmic ICs corresponding to the fetal cardiac activity

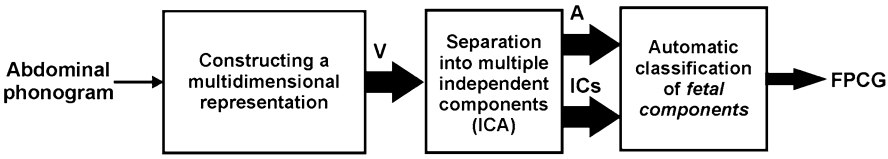

Fig. 3 Denoising procedure to extract the FPCG from the abdominal phonogram by using SCICA

and, thus, makes it possible to estimate the source of interest, i.e., the FPCG. These three stages are illustrated in Fig. 3 and described in Sects. 3.3.1, 3.3.2 and 3.3.3, respectively.

3.3.1 Mapping a Single-Channel Signal into a Multidimensional Representation

This first stage is implemented by using the method of delays (MD or dynamical embedding), which makes it possible to project an N_T-scalar time series $\{x_i\}_{i=1,\ldots,N_T}$ into a multichannel representation of the data [40]. This new representation, also known as the matrix of delays ($\mathbf{V}$), is built up by taking consecutive delay vectors of length m as $v_k = \{x_k, x_{k+1}, \ldots, x_{k+m-1}\}_{k=1,\ldots,N}$ and by using them as column vectors in the m-dimensional matrix $\mathbf{V} = \left[\boldsymbol{v}_1^T, \boldsymbol{v}_2^T, \ldots, \boldsymbol{v}_N^T\right]$. There, N corresponds to the number of delay vectors ($N = N_T - (m-1)$), and m corresponds to the embedding dimension ($m \geq fs/fl$), where fs is the sampling frequency (i.e., $fs = 500$ Hz) and fl is the lowest frequency component of interest in x_i.

In our work, by considering that the component with the lowest frequency in the FPCG is 10 Hz [41, 42], the value used for m has been 50. Regarding N, we empirically found that $N_T = 5000$ samples (i.e., 10 s) was good enough to ensure that the matrix of delays covered a quasi-stationary signal and then that ICA would converge. Thus, by using these parameters, we are certain that the multidimensional representation $\mathbf{V}$ ($m \times N$) is rich in temporal information about the fetal cardiac activity and, most importantly, that it is ready to be spanned by a convenient basis such as ICA.

3.3.2 Extraction of Multiple Independent Components

As mentioned in Sect. 2, a number of ICA implementations is currently available, and since the key point in each algorithm is the method used to numerically calculate statistical independence (e.g., higher-order statistics or time-structure-based algorithms), their performance on the ICs estimation will be different. In our research [19], we have studied two ICA implementations and found that the underlying components in the abdominal phonogram are better recovered by using

the Temporal Decorrelation Separation approach of TDSep [27] rather than by using the approach of FastICA [43].

In general words, the implementation of TDSep (1) defines independence by the absence of cross-correlations among the underlying components and (2) assumes that such components possess some temporal structure that, consequently, produce diagonal time-delayed correlation matrices, $R_\tau^{\mathbf{V}}$. Hence, TDSep analyzes the dependency structure of the multichannel representation, $\mathbf{V}$, by creating a set of square matrices and then by finding the joint diagonalizer of that set, which turns out to be the mixing matrix ($\hat{\mathbf{A}}$) mentioned in Eq. 6. To this end, TDSEP calculates a set of time-lagged correlation matrices of $\mathbf{V}$ by $R_\tau^{\mathbf{V}} = E\{\mathbf{V}[n]\,\mathbf{V}[n+\tau]\}$, where E represents expectation and τ $(= 0, 1, 2, \ldots, k)$ is the time lag. Then, since for independent components these matrices have to be diagonal, TDSep performs a joint diagonalization of $R_\tau^{\mathbf{V}}$ to estimate $\mathbf{A}$. Finally, after calculating $\mathbf{W}$ (which is the inverse of $\mathbf{A}$), it is possible to substitute it in Eq. 2 to estimate the constituent ICs in our matrix of delays $\mathbf{V}$.

In our research, knowing that the value of k defines the number of time lags and the quality of the separate ICs, we tested different k values and found that, in our dataset of abdominal phonograms, a value of $k = 1$ makes is possible to consistently process $\mathbf{V}$ and estimate the constituent ICs. As a result, TDSep estimates m ICs whose typical spectra are given by a well-defined single peak [19]. These ICs must be further analyzed to complete the denoising process as detailed in Sect. 3.3.3.

3.3.3 Automatic Classification of Fetal Independent Components

According to [32], when applying ICA to the matrix of delays $\mathbf{V}$, some of the estimate ICs will belong to the same independent process, which in our case can be described as either physiological or nonphysiological (e.g., the fetal cardiac activity, the maternal cardiac activity or line noise). Here, since we are only interested in retrieving the fetal cardiac information in the form of the FPCG, the denoising process will require identifying and grouping the ICs corresponding to the fetal subspace while discarding the others.

Before describing the classification process in this final stage of SCICA, it is imperative to mention two fundamental and consistent characteristics of the ICs recovered from the abdominal phonograms by TDSep; they are rhythmic and spectrally band-limited components as mentioned in [19, 44] and studied in [45]. These two characteristics are essential for this section, which describes a methodology for the automatic classification of the fetal cardiac ICs by using a couple of spectral features that are relatively easy to calculate, i.e., their rhythmicity and spectral content [20, 44, 45].

The procedure for this stage is conducted in four steps as follows:

(a) *Projecting ICs back to the measurement space* [17]: In this step, each IC is processed by $\mathbf{Y}^i = \boldsymbol{a}_i \boldsymbol{c}_i^T$, with $\boldsymbol{a}_i$ as the ith-column in the mixing matrix $\mathbf{A}$ (obtained by TDSep), $\boldsymbol{c}_i$ as the ith-IC, and $\mathbf{Y}^i$ as the resulting matrix of delays

for that IC ($i = 1, 2, \ldots, 50$). Next, $\mathbf{Y}^i$ is hankelized to produce the ith-projected IC (IC_p^i), by $\text{CI}_\text{p}^i = \frac{1}{50}\sum_{k=1}^{50} \mathbf{Y}^i_{k,(t+k-1)}$, where $t = 1, 2, \ldots, N$ [46].

(b) *Calculating spectral features*: This step quantifies the rhythmicity and frequency content of each IC_p^i as illustrated in Fig. 4 and described in the next paragraphs.

(i) *Frequency content of an* IC_p^i (S_I): This index is used as an indicator of the spectral content of the IC_p^i under analysis and is calculated using the Welch's method, with a Hanning window of 32 samples and an overlap of 50%. Then, from the characteristic band-limited spectrum obtained, $\hat{S}_x$, the frequency of its peak is taken as the index that represents the frequency content, S_I. Figure 4 presents an example of the S_I calculation for IC_p^{45} (one of the independent components presented in Sect. 3.4). The resulting trace, as can be observed, is band-limited and presents a well-defined single peak that is centered at $S_I = 27$ Hz.

(ii) *Rhythmicity of an* IC_p^i (R): This index is used as an indicator of the physiological generator driving the IC_p^i. As illustrated in Fig. 4, the calculation of R starts by generating a normalized envelope of the IC_p^i using the Hilbert transform. Next, the envelope autocorrelogram is generated and band-pass filtered from 0.7 to 3.1 Hz by a 10-order FIR filter (to reduce contributions from the maternal respiratory rhythm and from the harmonics of the maternal and fetal cardiac rhythms, respectively). Then, the filtered autocorrelogram is transformed into the frequency domain using the Welch's periodogram, with a Hanning window of 2018 samples and 50% overlap (which contains an average of eight fetal heart beats). Finally, from the resulting autospectrum, $\hat{S}_{xx}$, the frequency of the largest peak is used as the rhythmicity indicator, R. Figure 4 presents an example of the R calculation for IC_p^{45}. The resulting trace, as can be observed, presents a single rhythm that is centered at $R = 2.3$ Hz.

(c) *Selecting fetal components*: This third step starts by verifying whether the indexes R and S_I are between 1.7 and 3.0 Hz for the former and between 19.0 and 44.5 Hz for the latter, which are the intervals that our research has empirically identified as typical for the IC_p^is corresponding to the fetal cardiac process [44, 45]. In those cases where R and S_I disagree on the IC_p^i category, the S_I value has the highest priority, which means that, if S_I is in the fetal interval, then the component is classified as fetal cardiac without any further analysis. Alternatively, whenever both indexes R and S_I point at the component as a fetal IC_p^i, it is further analyzed to verify its stability (P) and identify if it is driven by a single biological rhythm (i.e., the fetal heart rate) or if it is contaminated by a second one (typically the maternal heart rate). Then, if the IC_p^i is found to be a stable component, it is classified as a fetal cardiac component. On the contrary, in those cases where the IC_p^i is found to be contaminated by a second biological rhythm (which happens to be the cardiac maternal rhythm), it is further analyzed to establish the level of contamination, and only the

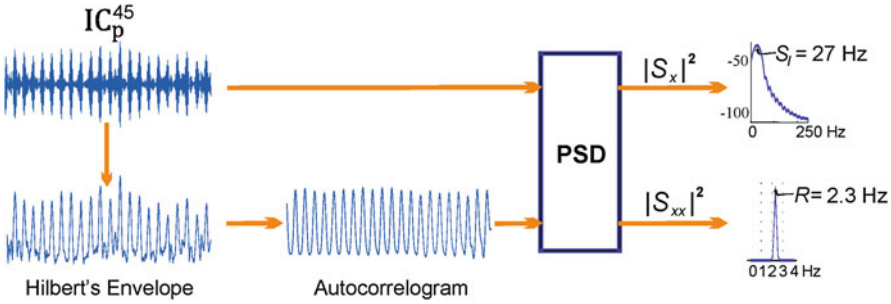

Fig. 4 Calculation of two spectral indexes (rhythmicity (R) and frequency content (S_I)) for automatic classification of the fetal cardiac components extracted by SCICA

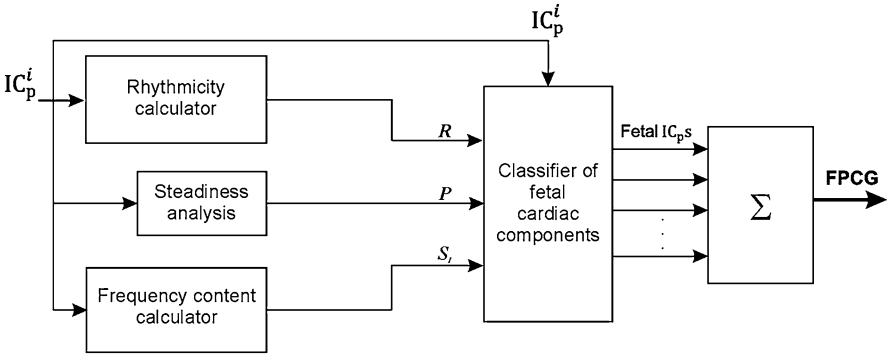

Fig. 5 Procedure for the identification and automatic classification of fetal cardiac components and construction of the FPCG trace in the third stage of SCICA

components where the contribution of the second rhythm is not important are classified as fetal cardiac components. This is done by calculating two Pearson's coefficients, one between the autocorrelogram and a sinusoid oscillating at the fetal heart rate and another between the autocorrelogram and a sinusoid oscillating at the maternal heart rate. Next, if the former Pearson's coefficient is larger than the latter (and S_I indicates that the component belongs to the fetal cardiac group), it is classified as fetal cardiac. Details of the complete version of this algorithm can be found in [20, 44], along with an evaluation of its performance. In this chapter, we are only describing the procedure that makes it suitable to classify the components that are more likely to belong to the fetal cardiac group.

(d) *Constructing the FPCG*: In this final step, the classified fetal cardiac IC_ps are summed for the construction of the FPCG trace as $FPCG = \sum$ fetal IC_ps [17].

Figure 5 presents the four steps followed in our methodology for classifying fetal IC_ps and constructing the trace corresponding to the FPCG.

3.4 Results

Figure 6 depicts the time and frequency representations of a 10 s segment of a noisy abdominal phonogram of subject 1 (40 weeks of gestational age) and 10 IC_ps (out of 50) separated and classified by our methodology for denoising the abdominal phonogram. From the abdominal phonogram, in the time domain, it is possible to distinguish a low-frequency component (with large amplitude between ± 2 V) and some peaks (indicated by upward arrows), but without any clear evidence of the fetal cardiac activity (i.e., the Fetal Heart Sounds (FHS)). In the frequency domain, the spectrum indicates that most of its power is concentrated below 75 Hz (> -30 dB), and the autospectrum indicates that four rhythms are present, with the strongest rhythm centered at 1.3 Hz.

Regarding the IC_ps, their frequency representations, as mentioned in Sect. 3.3.3, can be described as consistently given by (1) band-limited power spectra (i.e., a single-peak spectra) and (2) well-defined autospectra centered at a single dominant biological rhythm (below 4 Hz). These two characteristics made it possible for SCICA to automatically classify five of them as belonging to the fetal cardiac process ($IC^{42}{}_p$, $IC^{43}{}_p$, $IC^{44}{}_p$, $IC^{45}{}_p$, and $IC^{46}{}_p$). Such components, in the time domain, showed periodic activity almost every 0.45 s and appeared very clean (except for some disturbances indicated by a downward arrow), whereas in the frequency domain presented a power spectrum centered between 39 Hz ($IC^{42}{}_p$) and 21 Hz ($IC^{46}{}_p$), all of them with a rhythm centered at 2.3 Hz. The remaining components, $IC^{41}{}_p$, $IC^{47}{}_p$, $IC^{48}{}_p$, $IC^{49}{}_p$, and IC^{50}, although also depicted temporal structure (clearly indicated by the upward arrows in $IC^{49}{}_p$) and band-limited spectra, do not belong to the fetal cardiac process of interest in this study and, thus, were discarded during the classification stage as part of the denoising strategy followed by SCICA. At the end, as can be seen, among the 50 IC_ps extracted from this segment of abdominal phonogram in the second stage of SCICA, only five components were used to construct the trace corresponding to the fetal cardiac activity, i.e., the FPCG. This example illustrates one of the best cases, where the separate IC_ps were driven by a single biological rhythm (observed in both the temporal structure and autospectrum) that, detected by a "relatively" easy set of rules, successfully classified the fetal components of interest.

Figure 7 illustrates the time and frequency representations of a 10 s segment of a noisy abdominal phonogram of subject 1 (40 weeks of gestational age) and its denoised version (i.e., the FPCG with its two main heart sounds, S1 and S2) generated by SCICA. Complementary, as a reference signal, the abdominal ECG is included. The abdominal phonogram, as can be seen, is a noisy trace composed of different sources that unease the identification of the fetal information in both time and frequency domains. On the contrary, the denoised trace produced by SCICA (i.e., the FPCG) shows periodic activity at about every 0.45 s with amplitude of ± 1 V. In addition, such activity is temporally aligned with the fetal QRS complex in the abdominal ECG (indicated by a dotted vertical line), which confirms that this trace actually corresponds to the FPCG (where the two main heart sounds, S1 and S2, can be seen). Also, the time series shows that S1 has the highest amplitude and